Journal of Organometallic Chemistry 694 (2009) 2053–2060

Contents lists available at ScienceDirect

Journal of Organometallic Chemistry

journal homepage: www.elsevier.com/locate/jorganchem

Versatile coordination chemistry of rhodium complexes containing the bis(trimethylsilylmethyl)tellane ligand

Ludmila Vigo, Merja J. Poropudas, Pekka Salin, Raija Oilunkaniemi *, Risto S. Laitinen *

Department of Chemistry, University of Oulu, P.O. Box 3000, FI-90014 Oulu, Finland

ARTICLE INFO

Article history:
Received 10 January 2009
Received in revised form 30 January 2009
Accepted 3 February 2009
Available online 13 February 2009

Keywords:
Bis(trimethylsilylmethyl)tellane
Mononuclear rhodium complexes
Dinuclear rhodium complexes
Molecular Structure
X-ray diffraction
NMR spectroscopy

ABSTRACT

When $RhCl_3 \cdot 3H_2O$ was treated with an excess of $Te(CH_2SiMe_3)_2$, a mononuclear *mer*-$[RhCl_3\{Te(CH_2SiMe_3)_2\}_3]$ (**1**) was observed as the main product. By reducing the metal-to-ligand molar ratio, dinuclear $[Rh_2(\mu\text{-}Cl)_2Cl_4\{Te(CH_2SiMe_3)_2\}_4]$ (**2**) was obtained in addition to **1**. Further reduction of the metal-to-ligand ratio resulted in the formation of $[Rh_2(\mu\text{-}Cl)_2Cl_4(OHCH_2CH_3)\{Te(CH_2SiMe_3)_2\}_3]$ (**3**). The treatment of *mer*-$[RhCl_3(SMePh)_3]$ (**4**) with two equivalents of $Te(CH_2SiMe_3)_2$ affords a mixture of *mer*-$[RhCl_3\{Te(CH_2SiMe_3)_2\}_3]$ (**1**) and *mer*-$[RhCl_3\{Te(CH_2SiMe_3)_2\}_2(SMePh)]$ (**5**). All complexes **1**–**4** and **5** · ½EtOH were characterized by X-ray crystallography and ^{125}Te NMR spectroscopy, where appropriate. The definite assignment of the ^{125}Te chemical shifts enabled a plausible discussion of the assignment of some unknown resonances that were observed in the NMR spectra.

1. Introduction

There is only little information on the chemistry of rhodium complexes containing telluroether ligands (for some selected reviews, see Refs. [1–5]). One of the first examples was the reported synthesis of $[RhCl_3(TePh_2)_3]$ from $RhCl_3$ and diphenyl telluride [6], but no structural information was given. More recently, the existence of both *mer*- and *fac*-isomers of $[RhCl_3L_3]$ (L = 1,3-dihydrobenzo[*c*]tellurophene, tetrahydrotellurophene) complexes in solution was inferred based on NMR spectroscopic information [7,8].

Of the few known crystal structures of mononuclear rhodium complexes that contain telluroether ligands [9–13], $[RhCp^*L][PF_6]_2$ {L = $MeS(CH_2)_3Te((CH_2)_3SMe)$} is of special interest, since L acts as a tridentate ligand with one Te and two S donor atoms [13]. To our knowledge, no crystal structures of such hybrid rhodium complexes containing discrete thioether and telluroether ligands have hitherto been reported.

Bis(trimethylsilylmethyl)tellane ligand forms complexes with palladium(II), platinum(II), and ruthenium(II) centres that exhibit interesting stereochemical features [14–16]. In this paper, we are concerned with the reaction of $Te(CH_2SiMe_3)_2$ and $RhCl_3 \cdot 3H_2O$. We discuss the formation and structural characterization of *mer*-$[RhCl_3\{Te(CH_2SiMe_3)_2\}_3]$ (**1**), $[Rh_2(\mu\text{-}Cl)_2Cl_4\{Te(CH_2SiMe_3)_2\}_4]$ (**2**), and $[Rh_2(\mu\text{-}Cl)_2Cl_4(OHCH_2CH_3)\{Te(CH_2SiMe_3)_2\}_3]$ (**3**). We also describe the ligand substitution reaction in *mer*-$[RhCl_3(SMePh)_3]$ (**4**) by $Te(CH_2SiMe_3)_2$ that leads to the formation of **1** and hybrid *mer*-$[RhCl_3\{Te(CH_2SiMe_3)_2\}_2(SMePh)]$ (**5**). We have recently reported that the ligand substitution of SRPh (R = Ph, Me) in $[MCl_2(SRPh)_2]$ (M = Pt, Pd) by $Te(CH_2SiMe_3)_2$ affords a mixture of complexes containing $[MCl_2(SRPh)_2]$, $[MCl_2(SRPh)\{Te(CH_2SiMe_3)_2\}]$, and $[MCl_2\{Te(CH_2SiMe_3)_2\}_2]$ [17].

2. Experimental

2.1. General

$RhCl_3 \cdot 3H_2O$ (Aldrich), SMePh (Aldrich), ethanol (Altia), diethyl ether (Lab-Scan), and dichloromethane (Lab-Scan) were used as purchased and without further purification. $Te(CH_2SiMe_3)_2$ was prepared using the method described by Gysling et al. [14].

2.2. NMR spectroscopy

$^{13}C\{^1H\}$ and ^{125}Te NMR spectra were recorded on a Bruker DPX400 spectrometer operating at 100.61 MHz and 126.28 MHz, respectively. The typical respective spectral widths were 24.04 kHz and 126.58 kHz. The pulse widths were 11.00 μs and 10.00 μs, respectively. $^{13}C\{^1H\}$ pulse delay was 6.00 s and that for ^{125}Te was 1.60 s. $^{13}C\{^1H\}$ accumulations contained *ca.* 1000 transients and those for ^{125}Te 40000 transients. Tetramethylsilane was used as an internal standard for $^{13}C\{^1H\}$, and a saturated

* Corresponding authors. Tel.: +358 8 5531686; fax: +358 8 5531603 (R. Oilunkaniemi), tel.: +358 8 5531611; fax: +358 8 5531603 (R.S. Laitinen).
E-mail addresses: raija.oilunkaniemi@oulu.fi (R. Oilunkaniemi), risto.laitinen@oulu.fi (R.S. Laitinen).

0022-328X/$ - see front matter © 2009 Elsevier B.V. All rights reserved.
doi:10.1016/j.jorganchem.2009.02.001

Table 1
Crystal data and details of the structure determinations of *mer*-[$RhCl_3\{Te(CH_2SiMe_3)_2\}_3$] (**1**), [$Rh_2(\mu\text{-}Cl)_2Cl_4\{Te(CH_2SiMe_3)_2\}_4$] (**2**), [$Rh_2(\mu\text{-}Cl)_2Cl_4(OHCH_2CH_3)\{Te(CH_2SiMe_3)_2\}_3$] (**3**), *mer*-[$RhCl_3(SMePh)_3$] (**4**), and *mer*-[$RhCl_3\{Te(CH_2SiMe_3)_2\}_2(SMePh)$] · $\frac{1}{2}C_2H_5OH$ (**5** · ½EtOH).

	1	**2**	**3**	**4**	**5** · ½EtOH
Empirical formula	$C_{24}H_{66}Cl_3RhSi_6Te_3$	$C_{32}H_{88}Cl_6Rh_2Si_8Te_4$	$C_{26}H_{72}Cl_6ORh_2Si_6Te_3$	$C_{21}H_{24}Cl_3RhS_3$	$C_{24}H_{55}Cl_3O_{0.50}RhSSi_4Te_2$
Relative molecular mass	1115.37	1626.66	1370.70	581.84	960.56
Crystal system	Monoclinic	Monoclinic	Monoclinic	Monoclinic	Monoclinic
Space group	$P2_1/n$	$P2_1/c$	$P2_1/c$	$P2_1/c$	$P2_1/c$
a (Å)	14.722(3)	20.311(4)	11.276(2)	15.679(3)	16.871(3)
b (Å)	18.908(4)	14.151(3)	21.972(4)	10.278(2)	19.055(4)
c (Å)	17.334(4)	23.292(5)	21.429(4)	15.812(3)	13.202(3)
β (°)	98.25(3)	103.97(3)	97.83(3)	111.92(3)	100.29(3)
V (Å^3)	4775(2)	6496(2)	5260(2)	2363.9(8)	4176(1)
Z	4	4	4	4	4
$F(000)$	2184	3168	2672	1176	1900
$D_{calc.}$ (g cm^{-3})	1.551	1.663	1.731	1.635	1.528
μ(Mo Kα) (mm^{-1})	2.486	2.684	2.720	1.333	2.150
Crystal size (mm)	0.40 × 0.20 × 0.10	0.30 × 0.20 × 0.10	0.30 × 0.25 × 0.20	0.10 × 0.10 × 0.10	0.20 × 0.20 × 0.09
θ range (°)	3.00–26.00	3.02–26.00	2.94–26.00	2.60–26.00	3.04–26.00
No. of reflections collected	43539	64473	52072	31661	47992
No. of unique reflections	9250	12713	10304	4628	7707
No. of observed reflections[a]	7221	9481	8927	4365	6293
No. of parameters/restraints	353/0	503/6	416/0	256/0	342/2
$[R_{(int)}]$	0.0952	0.0862	0.0548	0.0400	0.0688
R_1[a,b]	0.0491	0.0494	0.0397	0.0236	0.0511
wR_2[a,b]	0.1243	0.1285	0.1018	0.0606	0.1266
R_1 (all data)[b]	0.0660	0.0734	0.0479	0.0258	0.0657
wR_2 (all data)[b]	0.1382	0.1478	0.1115	0.0616	0.1364
Goodness-of-fit on F^2	1.030	1.086	1.106	1.174	1.032
$\Delta\rho_{max,min}$ (e Å^{-3})	1.534, −1.441	2.574, −1.476	1.434, −1.388	0.479, −0.922	2.224, −1.173

[a] $I > 2\sigma(I)$.
[b] $R_1 = \sum ||F_o| - |F_c|| / \sum |F_o|$, $wR_2 = [\sum w(F_o^2 - F_c^2)^2 / \sum wF_o^4]^{1/2}$.

solution of Ph_2Te_2 in $CDCl_3$ as an external standard for ^{125}Te. The Te NMR spectra of the reaction solutions were recorded unlocked in EtOH. The $^{13}C\{^1H\}$ and ^{125}Te NMR spectra of the isolated complexes were recorded in $CDCl_3$ that served as an internal ^{2}H lock. Carbon chemical shifts (ppm) are reported relative to Me_4Si and tellurium chemical shifts relative to neat Me_2Te [δ (Me_2Te) = δ (Ph_2Te_2) + 422] [18].

2.3. X-ray crystallography

Diffraction data of **1**–**4** and **5** · ½EtOH were collected on a Nonius Kappa-CCD diffractometer at 120 K using graphite monochromated Mo Kα radiation (λ = 0.71073 Å; 55 kV, 25 mA). Crystal data and the details of structure determinations are given in Table 1.

Structures were solved by direct methods using SIR-92 [19] and refined using SHELXL-97 [20]. After the full-matrix least-squares refinement of the non-hydrogen atoms with anisotropic thermal parameters, the hydrogen atoms were placed in calculated positions in the OH group (O–H = 0.95 Å), in the aromatic rings (C–H = 0.95 Å), in the CH_3 groups (C–H = 0.98 Å) and in the CH_2 groups (C–H = 0.99 Å). The isotropic thermal parameters of the aromatic and methylene hydrogen atoms were fixed at 1.2 times and the methyl hydrogen atoms were fixed at 1.5 times to those of the corresponding carbon atom. The scattering factors for the neutral atoms were those incorporated with the programs. One trimethylsilyl group in complex **2** turned out to be disordered. In the refinement the disorder was taken into account by refining the site occupation factors of the two alternative orientations and constraining their sums to unity. Since the site occupation factors and thermal parameters of the disordered atoms correlate with each other, the thermal parameters of the corresponding pairs of atoms were restrained to be equal. A solvent molecule in the lattice of complex **5** was also severely disordered between two symmetry equivalent positions. This disorder was also resolved in a similar fashion.

2.4. Reaction of $RhCl_3 \cdot 3H_2O$ and $Te(CH_2SiMe_3)_2$

$RhCl_3 \cdot 3H_2O$ (0.0605 g; 0.2298 mmol) was dissolved in 2 ml of ethanol and $Te(CH_2SiMe_3)_2$ (0.2430 g; 0.8045 mmol) dissolved in 2 ml of ethanol was added into the resulting solution. (metal-to-ligand molar ratio of 1:3½). The reaction mixture was stirred at room temperature for 24 h. The resulting solution was cooled to −20 °C during which time orange-red crystals of *mer*-[$RhCl_3\{Te(CH_2SiMe_3)_2\}_3$] (**1**) were formed. Yield: 0.1462 g (57%). Anal. Calc. for $C_{24}H_{66}Cl_3RhSi_6Te_3$ (**1**): C, 25.84; H, 5.96. Found: C, 27.56; H, 6.33%.[1] ^{125}Te NMR: 406 ppm (d, $^1J_{Te\text{-}Rh}$ = 96 Hz, Te3), 369 ppm (d, $^1J_{Te\text{-}Rh}$ = 67 Hz, Te1, Te2) (intensity ratio 1:2; for the numbering of atoms, see Fig. 1).

When the reaction solution of $RhCl_3 \cdot 3H_2O$ (0.0605 g; 0.2298 mmol), and $Te(CH_2SiMe_3)_2$ (0.2560 g; 0.8476 mmol) was refluxed for two hours before concentration by evaporation, the yield of the orange-red crystals of *mer*-[$RhCl_3\{Te(CH_2SiMe_3)_2\}_3$] (**1**) was 0.2024 g (79%).

The reaction and workup of the solution were repeated using a metal-to-ligand molar ratio of 1:2½ [$RhCl_3 \cdot 3H_2O$ 0.0642 g (0.2438 mmol) and $Te(CH_2SiMe_3)_2$ 0.2063 g (0.6830 mmol)]. A mixture of orange-red crystals of *mer*-[$RhCl_3\{Te(CH_2SiMe_3)_2\}_3$] (**1**) and red crystals of [$Rh_2(\mu\text{-}Cl)_2Cl_4\{Te(CH_2SiMe_3)_2\}_4$] (**2**) was formed upon cooling the solution to −20 °C. Anal. Calc. for $C_{32}H_{88}Cl_6Rh_2Si_8Te_4$ (**2**): C, 23.63; H, 5.45. Found: C, 23.92; H, 5.65%. ^{125}Te NMR: 557 ppm (d, $^1J_{Te\text{-}Rh}$ = 102 Hz, Te1, Te2), 463 ppm (d, $^1J_{Te\text{-}Rh}$ = 74 Hz, Te3, Te4) (intensity ratio 1:1; for the numbering of atoms, see Fig. 2).

The reaction solution with the metal-to-ligand molar ratio of 1:1½ [$RhCl_3 \cdot 3H_2O$ 0.0331 g (0.126 mmol) and $Te(CH_2SiMe_3)_2$ 0.0564 g (0.187 mmol)] was refluxed for two hours. Upon partial evaporation of the solvent with subsequent cooling to −20 °C, dark

[1] The crystals of **1** were moist containing *ca.* 6% of solvent ethanol, as deduced by ^{13}C NMR. The calculated elemental analysis for this composition is C, 27.17; H, 6.42 that is consistent with the determined composition.

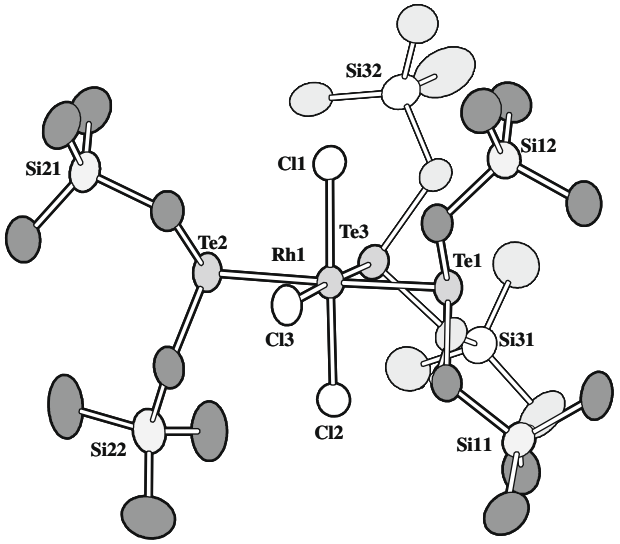

Fig. 1. Molecular structure of *mer*-[$RhCl_3\{Te(CH_2SiMe_3)_2\}_3$] (**1**) indicating the numbering of the atoms. The thermal ellipsoids have been drawn at 50% probability level. Hydrogen atoms have been omitted for clarity.

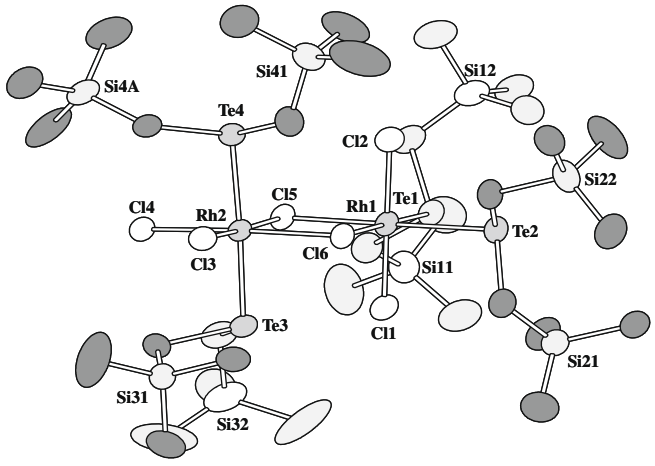

Fig. 2. Molecular structure of [$Rh_2(\mu\text{-}Cl)_2Cl_4\{Te(CH_2SiMe_3)_2\}_4$] (**2**) indicating the numbering of the atoms. The thermal ellipsoids have been drawn at 50% probability level. Hydrogen atoms have been omitted for clarity.

red crystals of [$Rh_2(\mu\text{-}Cl)_2Cl_4(OHCH_2CH_3)\{Te(CH_2SiMe_3)_2\}_3$] (**3**) were formed. Yield: 0.0469 g (37%). Anal. Calc. for $C_{26}H_{72}Cl_6ORh_2Si_6Te_3$ (**3**): C, 22.78; H, 5.29. Found: C, 23.01; H, 5.61%. ^{125}Te NMR: 683 ppm (d, $^1J_{Te\text{-}Rh}$ = 131 Hz, Te3), 560 ppm (d, $^1J_{Te\text{-}Rh}$ = 102 Hz, Te1, Te2) (intensity ratio 1:2; for the numbering of atoms, see Fig. 3).

2.5. Preparation of mer-[$RhCl_3(SMePh)_3$] (**4**)

$RhCl_3 \cdot 3H_2O$ (0.263 g, 1.00 mmol) and an excess of SMePh (0.752 g, 6.05 mmol) were refluxed in 10 ml of ethanol for 3.5 h. The dark red solution was cooled at room temperature and then to −20 °C. The resulting red crystals of *mer*-[$RhCl_3(SMePh)_3$] (**4**) were filtered off, washed several times with cold diethyl ether, and dried. Yield: 0.470 g (81%). Anal. Calc. for $RhCl_3S_3C_{21}H_{24}$ (**4**): C, 43.35; H, 4.16. Found: C, 43.46; H, 3.48%. $^{13}C\{^1H\}$ NMR: 124–128 ppm (m, phenyl groups), 19 ppm (s, C1, C2), 16 ppm (s, C3) (for the numbering of atoms, see Fig. 4).

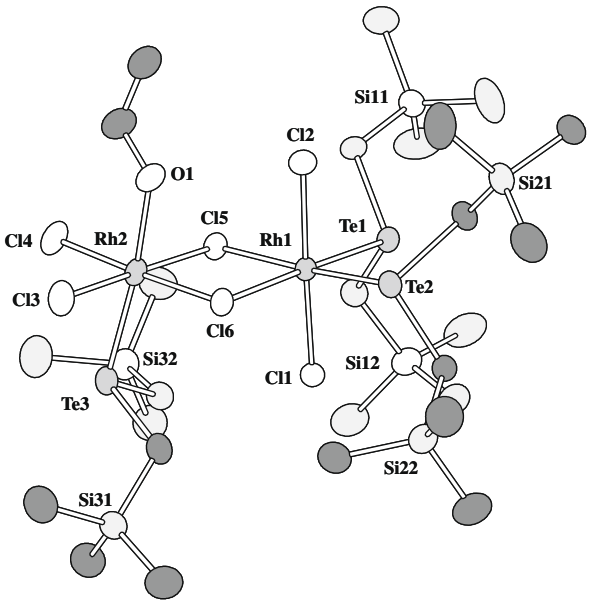

Fig. 3. Molecular structure of [$Rh_2(\mu\text{-}Cl)_2Cl_4(OHCH_2CH_3)\{Te(CH_2SiMe_3)_2\}_3$] (**3**) indicating the numbering of the atoms. The thermal ellipsoids have been drawn at 50% probability level. Hydrogen atoms have been omitted for clarity.

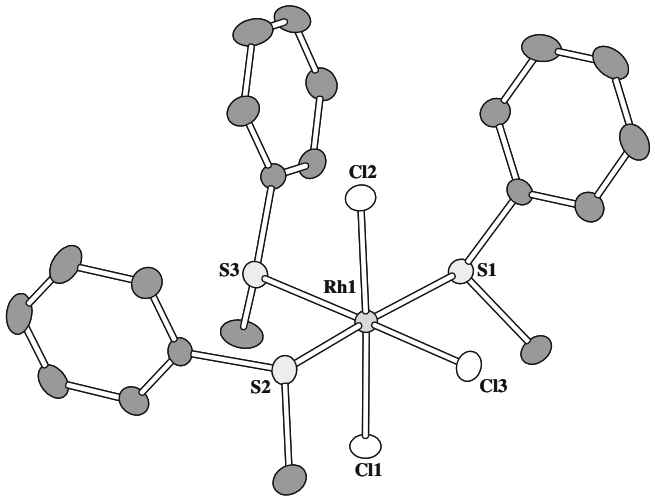

Fig. 4. Molecular structure of *mer*-[$RhCl_3(SMePh)_3$] (**4**) indicating the numbering of the atoms. The thermal ellipsoids have been drawn at 50% probability level. Hydrogen atoms have been omitted for clarity.

2.6. Reaction of mer-[$RhCl_3(SMePh)_3$] and $Te(CH_2SiMe_3)_2$

mer-[$RhCl_3(SMePh)_3$] (0.290 g, 0.50 mmol) was dissolved in 5 ml of ethanol and $Te(CH_2SiMe_3)_2$ (0.304 g; 1.00 mmol) was added into the resulting solution. The reaction mixture was stirred for an hour at room temperature and then concentrated by partial evaporation of the solvent. The crude product was filtered off, washed several times with cold diethyl ether, and recrystallized from dichloromethane. A mixture of orange-red crystals of *mer*-[$RhCl_3\{Te(CH_2SiMe_3)_2\}_2(SMePh)] \cdot \frac{1}{2}CH_3CH_2OH$ (**5** · ½EtOH) [^{125}Te NMR: 430 ppm (d, $^1J_{Te\text{-}Rh}$ = 75 Hz)], *mer*-[$RhCl_3\{Te(CH_2SiMe_3)_2\}_3$] (**1**) [406 ppm (d, $^1J_{Te\text{-}Rh}$ = 96 Hz), 369 ppm (d, $^1J_{Te\text{-}Rh}$ = 67 Hz) (intensity ratio 1:2], and *mer*-[$RhCl_3(SMePh)_3$] (**4**) was obtained upon cooling the solution to −20 °C.

3. Results and discussion

3.1. The reaction of $RhCl_3 \cdot 3H_2O$ and $Te(CH_2SiMe_3)_2$

The formation of the complexes and the product distribution in the reaction of $RhCl_3 \cdot 3H_2O$ and $Te(CH_2SiMe_3)_2$ are dependent on the initial molar ratio of the reactants.

3.1.1. Metal-to-ligand molar ratio above 1:3½

When the reaction mixture employing the metal-to-ligand molar ratio above 1:3½ was carried out by stirring the reactants at room temperature, the ^{125}Te NMR spectrum of the reaction solution showed four resonances at 420 ppm ($^1J_{Te\text{-}Rh}$ = 80 Hz), 406 ($^1J_{Te\text{-}Rh}$ = 96 Hz, $^2J_{Te\text{-}Te}$ = 790 Hz), 369 ppm ($^1J_{Te\text{-}Rh}$ = 67 Hz, $^2J_{Te\text{-}Te}$ = 790 Hz), and 294 ppm ($^1J_{Te\text{-}Rh}$ = 62 Hz.). Upon refluxing the reaction mixture, the resonance at 420 ppm disappeared, and the relative intensity of that at 294 ppm became smaller.

The resonances at 406 and 369 ppm showed a relative intensity ratio of 1:2 in spectra of both room temperature and refluxed reaction mixtures. They were assigned to the mononuclear *mer*-$[RhCl_3\{Te(CH_2SiMe_3)_2\}_3]$ (**1**) complex based on the X-ray structure determination of the orange-red crystals that were obtained upon crystallization. This assignment was verified by redissolving the crystals in $CDCl_3$ and re-recording the ^{125}Te NMR spectrum.

The molecular structure of **1** is shown in Fig. 1. The selected bond parameters are presented in Table 2. The lattice of **1** is built up of discrete molecules with the coordination sphere of rhodium a slightly distorted octahedron. The two 'axial' Rh–Te bonds Rh1–Te1 and Rh1–Te2 show the lengths of 2.6129(7) and 2.6439(7) Å, respectively. The 'equatorial' bond Rh1–Te3 is somewhat shorter and shows the length of 2.5733(7) Å. The relative bond lengths are consistent with the stronger *trans*-influence of tellurium compared to that of chlorine and is also reflected by the smaller $^1J_{Te\text{-}Rh}$ coupling constant of the more intense resonance at 369 ppm compared to that of the less intense resonance at 406 ppm.

The stronger *trans*-influence of tellurium than that of chlorine is also reflected by the Rh–Cl distances. Rh1–Cl1 and Rh1–Cl3 that are in *trans*-position to each other show shorter lengths of 2.362(2) and 2.353(2) Å, respectively, than Rh1–Cl3 of 2.381(1) Å that is in *trans*-position with respect to Te3.

The tentative assignment of the resonances at 420 ppm ($^1J_{Te\text{-}Rh}$ = 80 Hz) and 294 ppm ($^1J_{Te\text{-}Rh}$ = 62 Hz) will be discussed below (see Section 3.3 *Tentative Assignment of Unknown Resonances*).

3.1.2. Metal-to-ligand molar ratio 1:2½

Upon decreasing the relative amount of $Te(CH_2SiMe_3)_2$, two new major resonances of approximately equal intensity were observed at 557 ($^1J_{Te\text{-}Rh}$ = 102 Hz) and 463 ppm ($^1J_{Te\text{-}Rh}$ = 74 Hz) in

Table 2
Selected bond lengths (Å) and angles (°) in *mer*-$[RhCl_3\{Te(CH_2SiMe_3)_2\}_3]$ (**1**), $[Rh_2(\mu\text{-}Cl)_2Cl_4\{Te(CH_2SiMe_3)_2\}_4]$ (**2**), and $[Rh_2(\mu\text{-}Cl)_2Cl_4(OHCH_2CH_3)\{Te(CH_2SiMe_3)_2\}_3]$ (**3**).

1		**2**		**3**	
Rh1–Te1	2.6129(7)	Rh1–Te1	2.5501(8)	Rh1–Te1	2.5539(6)
Rh1–Te2	2.6439(7)	Rh1–Te2	2.5631(9)	Rh1–Te2	2.5539(8)
Rh1–Te3	2.5733(7)	Rh1–Cl1	2.348(2)	Rh1–Cl1	2.333(1)
Rh1–Cl1	2.362(2)	Rh1–Cl2	2.349(2)	Rh1–Cl2	2.364(1)
Rh1–Cl2	2.353(2)	Rh1–Cl5	2.417(2)	Rh1–Cl5	2.428(1)
Rh1–Cl3	2.381(1)	Rh1–Cl6	2.424(2)	Rh1–Cl6	2.454(1)
		Rh2–Te3	2.6330(8)	Rh2–Te3	2.5192(7)
Te1–Rh1–Te2	175.03(2)	Rh2–Te4	2.6359(8)	Rh2–O1	2.174(4)
Te1–Rh1–Te3	93.21(2)	Rh2–Cl3	2.325(2)	Rh2–Cl3	2.321(1)
Te1–Rh1–Cl1	89.24(4)	Rh2–Cl4	2.316(2)	Rh2–Cl4	2.328(1)
Te1–Rh1–Cl2	90.75(4)	Rh2–Cl5	2.389(2)	Rh2–Cl5	2.380(1)
Te1–Rh1–Cl3	88.60(4)	Rh2–Cl6	2.391(2)	Rh2–Cl6	2.369(1)
Te2–Rh1–Te3	91.09(2)				
Te2–Rh1–Cl1	88.29(4)	Te1–Rh1–Te2	88.26(2)	Te1–Rh1–Te2	94.00(2)
Te2–Rh1–Cl2	91.95(4)	Te1–Rh1–Cl1	86.00(5)	Te1–Rh1–Cl1	87.64(4)
Te2–Rh1–Cl3	87.20(4)	Te1–Rh1–Cl2	92.96(5)	Te1–Rh1–Cl2	92.33(4)
Te3–Rh1–Cl1	89.62(4)	Te1–Rh1–Cl5	93.45(4)	Te1–Rh1–Cl5	92.89(3)
Te3–Rh1–Cl2	87.31(4)	Te1-Rh1–Cl6	178.23(4)	Te1–Rh1–Cl6	175.36(3)
Te3–Rh1–Cl3	177.10(4)	Te2–Rh1–Cl1	91.83(5)	Te2–Rh1–Cl1	94.22(4)
Cl1–Rh1–Cl2	176.93(5)	Te2–Rh1–Cl2	88.22(5)	Te2–Rh1–Cl2	83.27(4)
Cl1–Rh1–Cl3	92.67(5)	Te2–Rh1–Cl5	178.11(4)	Te2–Rh1–Cl5	170.89(3)
Cl2–Rh1–Cl3	90.40(5)	Te2–Rh1–Cl6	92.85(4)	Te2–Rh1–Cl6	89.58(3)
		Cl1–Rh1–Cl2	178.95(6)	Cl1–Rh1–Cl2	177.47(5)
		Cl1–Rh1–Cl5	89.10(6)	Cl1–Rh1–Cl5	90.02(5)
		Cl1–Rh1–Cl6	92.58(6)	Cl1–Rh1–Cl6	89.16(5)
		Cl2–Rh1–Cl5	90.88(6)	Cl2–Rh1–Cl5	90.50(5)
		Cl2–Rh1–Cl6	88.46(6)	Cl2–Rh1–Cl6	91.01(5)
		Cl5–Rh1–Cl6	85.47(5)	Cl5–Rh1–Cl6	83.86(4)
		Te3–Rh2–Te4	177.92(2)	Te3–Rh2–O1	173.8(1)
		Te3–Rh2–Cl3	89.50(4)	Te3–Rh2–Cl3	83.72(4)
		Te3–Rh2–Cl4	90.62(5)	Te3–Rh2–Cl4	82.54(5)
		Te3–Rh2–Cl5	93.60(4)	Te3–Rh2–Cl5	96.70(4)
		Te3–Rh2–Cl6	86.21(5)	Te3–Rh2–Cl6	99.51(4)
		Te4–Rh2–Cl3	90.31(4)	O1–Rh2–Cl3	90.91)
		Te4–Rh2–Cl4	87.32(5)	O1–Rh2–Cl4	94.7(1)
		Te4–Rh2–Cl5	86.70(4)	O1–Rh2–Cl5	88.8(1)
		Te4–Rh2–Cl6	95.86(5)	O1–Rh2–Cl6	83.5(1)
		Cl3–Rh2–Cl4	91.94(6)	Cl3–Rh2–Cl4	91.36(5)
		Cl3–Rh2–Cl5	175.86(6)	Cl3–Rh2–Cl5	177.68(5)
		Cl3–Rh2–Cl6	90.63(5)	Cl3–Rh2–Cl6	90.90(5)
		Cl4–Rh2–Cl5	90.77(6)	Cl4–Rh2–Cl5	90.96(5)
		Cl4–Rh2–Cl6	175.90(6)	Cl4–Rh2–Cl6	177.10(5)
		Cl5–Rh2–Cl6	86.84(5)	Cl5–Rh2–Cl6	86.77(4)

addition to those of **1**. The crystallization of the reaction solution afforded a mixture of two sets of crystals: orange-red crystals of **1** and red crystals that upon crystal structure determination was shown to be dinuclear $[Rh_2(\mu\text{-}Cl)_2Cl_4\{Te(CH_2SiMe_3)_2\}_4]$ (**2**).

The molecular structure of **2** is shown in Fig. 2 and the selected bond parameters in Table 2. The lattice of **2** is built up of discrete dinuclear complexes in which the two rhodium centers are linked by two bridging chloride ligands. Both rhodium centers show a slightly distorted octahedral coordination environment. Rh1 has two equatorial tellane ligands in *cis*-positions to each other and two axial chlorido ligands in *trans*-positions to each other. By contrast, Rh2 shows two *trans*-tellane ligands in the axial positions and two equatorial *cis*-chlorido ligands.

Similar structures have been reported for $[Rh_2(\mu\text{-}X)_2X_4(PR_3)_4]$ (X = Cl, Br; R = Et, ^{n}Bu) containing phosphine ligands [21,22]. The isomerism of the dinuclear complexes was rationalized by Cotton et al. [21], who concluded that the preferred isomers obeyed two principles: (1) no μ-ligand should have both of its bonds weakened by the strong *trans*-influence of the phosphine ligand, and (2) for steric reasons two phosphine ligands should not occupy adjacent axial positions on the two rhodium atoms. However, *cis*-*cis* arrangement has been reported for $[Rh_2(\mu\text{-}Br)_2Br_4(PMe_3)_4]$ with sterically less demanding PMe_3 ligands [29].

The Rh–Te bonds Rh1–Te1 and Rh1–Te2 that are in *cis*-positions to each other show lengths of 2.5501(8) and 2.5631(9) Å, respectively. They are shorter than the Rh2–Te3 and Rh2–Te4 bonds [2.6330(8) and 2.6359(8) Å, respectively] that are a part of the *trans*-tellane arrangement. These bond lengths again demonstrate the relative strengths of the *trans*-influence of the tellurium and chlorine atoms that is also reflected by the bridging Rh–Cl bond lengths. The Rh1–Cl5 and Rh1–Cl6 bonds that are in *trans*-positions to tellurium atoms show lengths of 2.417(2) and 2.424(2) Å, respectively, while Rh2–Cl5 and Rh2–Cl6 that are in *trans*-positions to chlorine show slightly shorter lengths of 2.380(2) and 2.369(2) Å, respectively. All Rh–Cl distances are consistent with those reported for related $[Rh_2(\mu\text{-}Cl)_2Cl_4(PR_3)_4]$ (R = Et, ^{n}Bu) complexes [21].

The two ^{125}Te resonances in the NMR spectrum of the reaction mixture can now be assigned. That at 557 ppm ($^1J_{Te\text{-}Rh}$ = 102 Hz) is due to the two tellurium atoms in relative *cis*-positions (Te1 and Te2, see Fig. 2), and the resonance at 463 ppm ($^1J_{Te\text{-}Rh}$ = 74 Hz) is consequently assigned to two tellurium atoms in the relative *trans*-positions (Te3 and Te4). The coupling constants are consistent with the relative strengths of the *trans*-influence of tellurium and chlorine.

The relative intensities of the resonances in the reaction mixture indicate that it contains *ca.* 60 mol-% of **2** and 40 mol-% of **1**.

3.1.3. Metal-to-ligand molar ratio of 1:1½

When the relative amount of the ligand was reduced even further (metal-to-ligand molar ratio of 1:1½), the ^{125}Te NMR spectrum of the reaction mixture exhibited two doublets at 683 ppm ($^1J_{Te\text{-}Rh}$ = 131 Hz) and 560 ppm ($^1J_{Te\text{-}Rh}$ = 102 Hz) with the relative intensity ratio of 1:2.

The crystallization of the reaction solution afforded dark red crystals of $[Rh_2(\mu\text{-}Cl)_2Cl_4(OHCH_2CH_3)\{Te(CH_2SiMe_3)_2\}_3]$ (**3**). The molecular structure of **3** is shown in Fig. 3 and the selected bond parameters in Table 2.

The lattice of **3** is also built up with discrete dinuclear complexes in which the two octahedral rhodium centers are linked with bridging chlorido ligands. Rh1 shows two *cis*-tellane ligands in the equatorial plane in a similar fashion to **2**. Rh2 has one axial tellane ligand with a solvent ethanol molecule coordinated to the metal in the *trans*-position. Like in the case of **2**, the chlorido ligands Cl3, Cl4, Cl5, and Cl6 lie in the equatorial plane, while Cl1 and Cl2 occupy axial positions (see Figs. 2 and 3).

The Rh–Te bond lengths Rh1–Te1 and Rh1–Te2 involving the *cis*-tellane arrangements [2.5539(6) and 2.5539(8) Å, respectively] agree well with those of **2**. The Rh2–Te3 bond of 2.5192(7) Å is somewhat shorter and is consistent with the weaker *trans*-influence of oxygen compared to that of chlorine. When comparing the Rh–Cl bond lengths in **2** and **3**, it can be concluded that the relative lengths of the corresponding bonds agree well with each other.

3.2. Ligand substitution of mer-[$RhCl_3(SMePh)_3$] by $Te(CH_2SiMe_3)_2$

mer-$[RhCl_3(SMePh)_3]$ (**4**) was prepared with good yield by refluxing $RhCl_3{\cdot}3H_2O$ with an excess of SMePh in ethanol. Red crystals of **4** were formed upon cooling the reaction solution. The $^{13}C\{^1H\}$ NMR spectrum of **4** that was recorded, when the crystals of **4** were dissolved in $CDCl_3$ displayed two sets of resonances with the intensity ratio of 2:1, as expected for the *mer*-isomer containing two MePhS ligands in mutual *trans*-positions with each other and one ligand in *cis*-position with respect to both of them. Thus, the resonances at 19 and 16 ppm (intensity ratio 2:1) were assigned to the two equivalent methyl groups of the ligands in *trans*-position with respect to each other and to the methyl group of the ligand in the *cis*-position, respectively. The resonances of aromatic carbon atoms were found in the range 124–128 ppm. Their number and intensity were also consistent with the presence of the *mer*-isomer.

The crystal structure determination showed that **4** is *mer*-$[RhCl_3(SMePh)_3]$ that is composed of discrete complexes in which the coordination sphere around rhodium is a slightly distorted octahedron (see Fig. 4). The selected bond lengths and angles are shown in Table 3.

The Rh–S bond lengths span a range of 2.3561(6)–2.3623(7) Å. They are in agreement with the Rh–S distances reported for *mer*-$[RhCl_3(SMe_2)_3]$ [2.3283(8)–2.3660(7) Å] [23], *mer*-$[RhCl_3(SC_4H_8)_3]$ [2.333(1)–2.363(1) Å] [24], and *mer*-$[RhCl_3(SC_8H_8)_3]$ [2.330(1)–2.369(1) Å] [25]. The Rh–Cl bond lengths range 2.336(1)–2.359(1) Å, again in agreement with those of 2.3350(7)–2.3609(7) Å [23], 2.341(1)–2.355(1) Å [24], and 2.333(2)–2.359(1) [25] observed in *mer*-$[RhCl_3(SMe_2)_3]$, *mer*-$[RhCl_3(SC_4H_8)_3]$, and *mer*-$[RhCl_3(SC_8H_8)_3]$, respectively. The *trans*-influence of chlorine and sulfur seems to be of comparable strength with possibly that

Table 3
Selected bond lengths (Å) and angles (°) in *mer*-$[RhCl_3(SMePh)_3]$ (**4**) and *mer*-$[RhCl_3\{Te(CH_2SiMe_3)_2\}_2(SMePh)] \cdot \frac{1}{2}C_2H_5OH$ (**5** · ½EtOH).

4		**5**	
Rh1–S1	2.3561(6)	Rh1–Te1	2.6479(8)
Rh1–S2	2.3623(7)	Rh1–Te2	2.6383(9)
Rh1–S3	2.3584(6)	Rh1–S1	2.336(2)
Rh1–Cl1	2.359(1)	Rh1–Cl1	2.356(2)
Rh1–Cl2	2.336(1)	Rh1–Cl2	2.333(2)
Rh1–Cl3	2.348(1)	Rh1–Cl3	2.345(2)
S1–Rh1–S2	172.99(2)	Te1–Rh1–Te2	173.15(2)
S1–Rh1–S3	92.12(2)	Te1–Rh1–S1	98.37(5)
S1–Rh1–Cl1	88.71(3)	Te1–Rh1–Cl1	88.84(4)
S1–Rh1–Cl2	92.86(3)	Te1–Rh1–Cl2	85.59(5)
S1–Rh1–Cl3	92.76(2)	Te1–Rh1–Cl3	90.35(5)
S2–Rh1–S3	94.21(2)	Te2–Rh1–S1	88.20(5)
S2–Rh1–Cl1	94.20(3)	Te2–Rh1–Cl1	92.92(4)
S2–Rh1–Cl2	84.46(3)	Te2–Rh1–Cl2	90.35(5)
S2–Rh1–Cl3	80.78(2)	Te2–Rh1–Cl3	87.79(5)
S3–Rh1–Cl1	90.69(2)	S1–Rh1–Cl1	91.80(6)
S3–Rh1–Cl2	87.23(2)	S1–Rh1–Cl2	84.68(7)
S3–Rh1–Cl3	174.39(2)	S1–Rh1–Cl3	175.73(6)
Cl1–Rh1–Cl2	177.44(2)	Cl1–Rh1–Cl2	176.24(7)
Cl1–Rh1–Cl3	92.18(2)	Cl1–Rh1–Cl3	89.84(5)
Cl2–Rh1–Cl3	89.76(2)	Cl2–Rh1–Cl3	93.76(6)

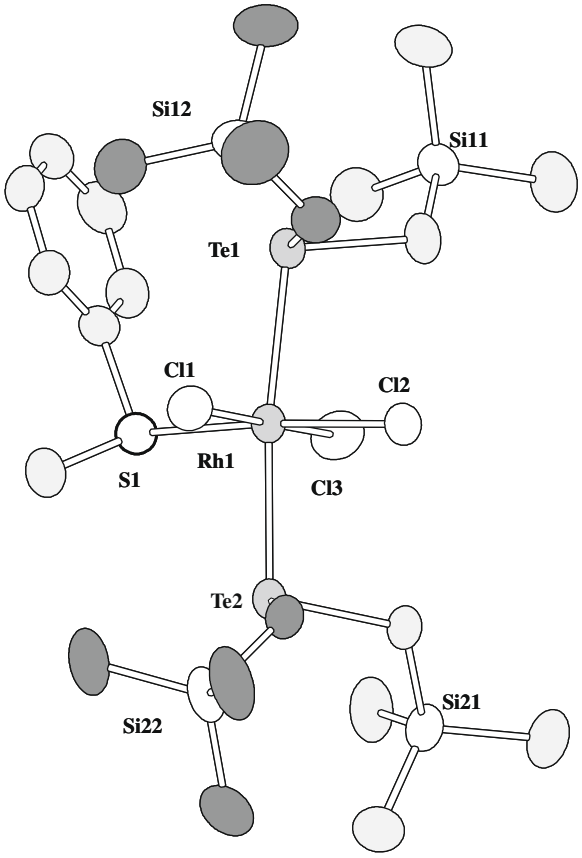

Fig. 5. Molecular structure of *mer*-[$RhCl_3${$Te(CH_2SiMe_3)_2$}$_2$(SMePh)] · ½CH_3CH_2OH (**5** · ½EtOH) indicating the numbering of the atoms. The thermal ellipsoids have been drawn at 50% probability level. Hydrogen atoms and the disordered solvent molecule have been omitted for clarity.

Table 4
The observed and calculated ^{125}Te chemical shifts of mononuclear [$RhCl_x${ERR'}$_{6-x}$] (E = S, Te; R, R′ = alkyl groups) complexes.

Complex	χ_t[a]	$\Sigma\chi_c$[b]	δ_{obs} (ppm)	δ_{calc}[c] (ppm)
[$RhCl_3${$Te(CH_2SiMe_3)_2$}$_2$(SMePh)][d]	2.10	12.06	430	422
fac-[$RhCl_3(TeC_4H_8)_3$][e]	3.16	10.52	429	413
fac-[$RhCl_3${$Te(CH_2SiMe_3)_2$}$_3$][e]	3.16	10.52	420	413
mer-[$RhCl_3(TeC_4H_8)_3$][e]	3.16	10.52	416[f]	413
mer-[$RhCl_3${$Te(CH_2SiMe_3)_2$}$_3$][e]	3.16	10.52	406	413
mer-[$RhCl_3${$Te(CH_2SiMe_3)_2$}$_3$][d]	2.10	11.58	369	381
mer-[$RhCl_3(TeC_4H_8)_3$][d]	2.10	11.58	359[f]	381
trans-[$RhCl_2${$Te(CH_2SiMe_3)_2$}$_4$][d]	2.10	10.52	294	290

[a] Pauling electronegativities [26] of the donor atoms in *trans*-position to the observed ^{125}Te nuclei.
[b] The sum of Pauling electronegativities [26] of the four *cis*-donor atoms.
[c] See Eq. (1).
[d] *trans*-**Te**–Rh–Te arrangement.
[e] *trans*-**Te**–Rh–Cl arrangement (the observable ^{125}Te nuclei are indicated in bold).
[f] Ref. [8].

of sulfur slightly stronger. Therefore, there are no clear trends in the relative lengths of the Rh–S and Rh–Cl bonds with respect to the identity of the ligand that lies *trans* to it.

The treatment of *mer*-[$RhCl_3(SMePh)_3$] (**4**) with two equivalents of $Te(CH_2SiMe_3)_2$ affords a mixture of *mer*-[$RhCl_3${$Te(CH_2SiMe_3)_2$}$_3$] (**1**) and *mer*-[$RhCl_3${$Te(CH_2SiMe_3)_2$}$_2$(SMePh)] (**5**). Some unreacted **4** is also found in the reaction solution. The complex **5** exhibits a ^{125}Te resonance at 430 ppm ($^1J_{Te\text{-}Rh}$ = 75 Hz). The $^1J_{Te\text{-}Rh}$ coupling constant is consistent with that of mutually *trans*-tellane ligands in **1**. The reaction of *mer*-[$RhCl_3(SMePh)_3$] (**4**) and $Te(CH_2SiMe_3)_2$ is similar to the ligand substitution of SRPh (R = Ph, Me) in [$MCl_2(SRPh)_2$] (M = Pt, Pd) by $Te(CH_2SiMe_3)_2$ that affords a mixture of complexes containing [$MCl_2(SRPh)_2$], [MCl_2(SRPh){$Te(CH_2SiMe_3)_2$}], and [MCl_2{$Te(CH_2SiMe_3)_2$}$_2$] [17].

The recrystallization of the crude product from dichloromethane enabled the visual separation of orange-red crystals from the

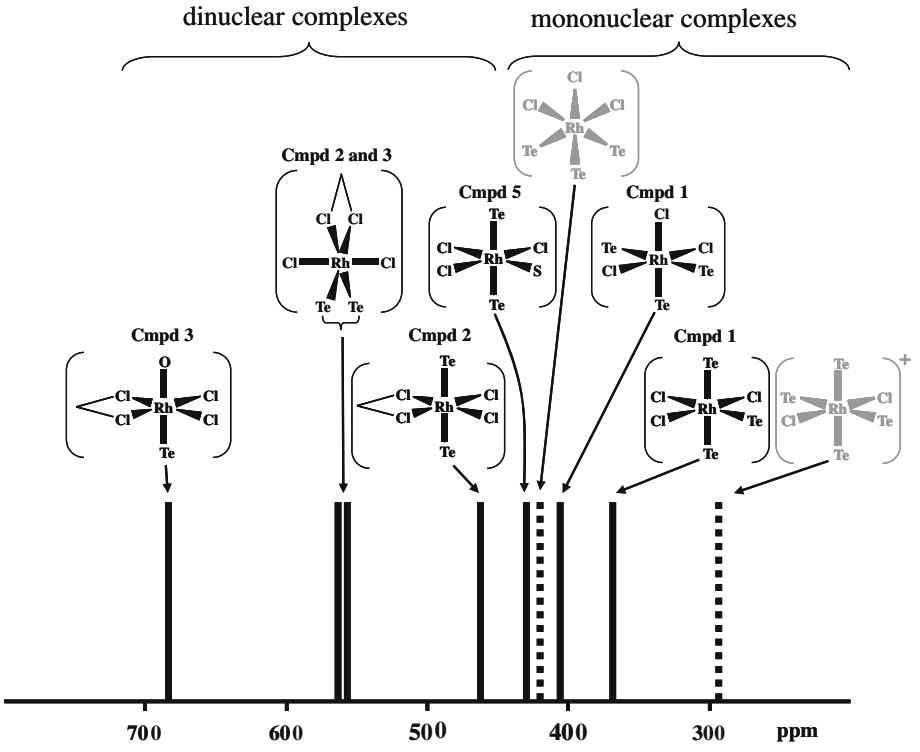

Fig. 6. The assignment of resonances in the ^{125}Te chemical shifts of mononuclear and dinuclear bis(trimethylsilylmethyl)tellanerhodium complexes. Solid lines together with black structural formulae indicate definitely assigned chemical shifts and the fragmented lines with gray structural formulae indicate tentatively assigned chemical shifts.

solid mixture that upon crystal structure determination turned out to be *mer*-[$RhCl_3${$Te(CH_2SiMe_3)_2$}$_2$(SMePh)] · ½CH_3CH_2OH (**5** · ½EtOH) with the two tellane ligands in *trans*-positions with respect to each other. The molecular structure of **5** is shown in Fig. 5 and the selected bond lengths in Table 3. The Rh–S bond is *trans* to the chlorine atom and shows the length of 2.336(2) Å, which is consistent with other Rh–S bonds considered in this work. The Rh1–Te1 and Rh1–Te2 bonds of 2.6479(8) Å and 2.6383(9) Å are of the comparable length to the Rh2–Te3 and Rh2–Te4 in **2** that are also in mutual *trans*-positions to each other.

3.3. Tentative assignment of unknown resonances

The definite assignment of ^{125}Te resonances to complexes **1**–**3** and **5** enables discussion of the tentative assignment of the two ^{125}Te resonances at 420 and 294 ppm that were observed in the reaction of $RhCl_3 \cdot 3H_2O$ and $Te(CH_2SiMe_3)_2$ (metal-to-ligand ratio of 1:3½).

The ^{125}Te chemical shifts of the complexes **1**–**3** and **5** have been summarized in Fig. 6 together with the unknown resonances. It can be seen that the ^{125}Te chemical shifts of mononuclear complexes occur at low frequencies (below 450 ppm), whereas those of the dinuclear complexes are found at higher frequencies (above 450 ppm).

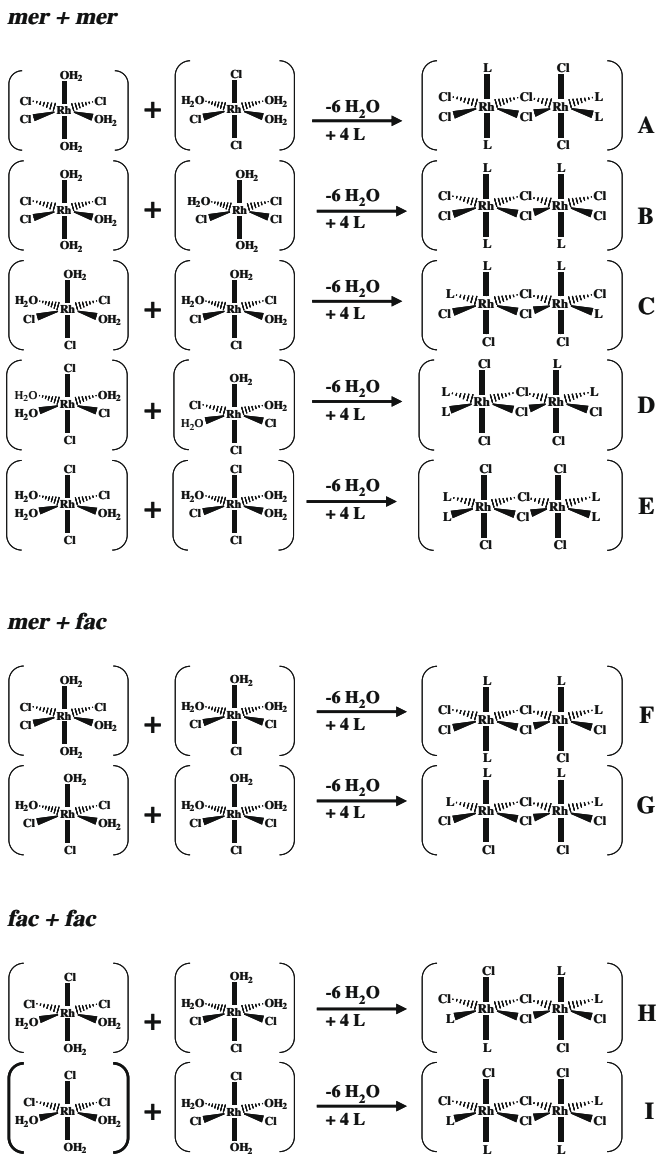

Fig. 7. The formation of the nine possible isomers of $[Rh_2Cl_6L_4]$ (**A**–**I**) from *mer*- and *fac*-isomers of $[RhCl_3(OH_2)_3]$.

The resonance at 420 ppm ($^1J_{Te\text{-}Rh}$ = 80 Hz) can be assigned to *fac*-[$RhCl_3${$Te(CH_2SiMe_3)_2$}$_3$]. It is seen from Fig. 6 that this resonance is found in the region of mononuclear complexes. The presence of both the *mer*- and *fac*-isomers in solution has been reported for [$RhCl_3(TeC_4H_8)_3$] [8] (*mer*-isomer: δ = 416 ppm, $^1J_{Te\text{-}Rh}$ = 95 Hz; δ = 359 ppm, $^1J_{Te\text{-}Rh}$ = 72 Hz; *fac*-isomer δ = 429 ppm, $^1J_{Te\text{-}Rh}$ = 92 Hz) and [$RhCl_3(TeC_8H_8)_3$] [7] (*mer*-isomer: δ = 620 ppm, $^1J_{Te\text{-}Rh}$ = 70 Hz; δ = 581 ppm, $^1J_{Te\text{-}Rh}$ = 70 Hz; *fac*-isomer δ = 592 ppm, $^1J_{Te\text{-}Rh}$ = 90 Hz.). The ^{125}Te NMR spectroscopic data for the two *mer*-isomers are in agreement with those for **1**. Those for the two *fac*-isomers are also consistent with the assignment of the resonance at 420 ppm to *fac*-[$RhCl_3${$Te(CH_2SiMe_3)_2$}$_3$].

It can also be deduced from Fig. 6 that the resonance at 294 ppm is due to a tellane ligand in a mononuclear complex. The appearance of only one resonance indicates that if there are more than one tellane ligand coordinated to rhodium, they all must be equivalent, The small $^1J_{Te\text{-}Rh}$ coupling constant of 62 Hz implies that there must be pairs of tellane ligands that are in *trans*-positions with respect to each other. Furthermore, there was an excess of ligand in the reaction solution that gave rise to the species displaying this resonance. Therefore, this complex could be expected to be tellane-rich.

In complexes containing similar tellane ligands, *i.e.* **1**, **5**, *fac*-[$RhCl_3${$Te(CH_2SiMe_3)_2$}$_3$], *mer*- and *fac*-isomers [$RhCl_3(TeC_4H_8)_3$] [8], the ^{125}Te chemical shifts are dependent on the Pauling electronegativities of the donor atoms. Because of the significance of the *trans*-influence, the electronegativity of the donor atom in the *trans*-position to the observed ^{125}Te nucleus is considered separately from the sum of the electronegativities of the four donor atoms in *cis*-positions. The least-squares fit of the definitely assigned chemical shifts results in the following relationship:

$$\delta(^{125}\mathrm{Te}) = 116 \cdot \chi_t + 85 \cdot \sum \chi_c - 851 \qquad (1)$$

where χ_t is the Pauling electronegativity [26] of the donor atom in *trans*-position to the observed ^{125}Te nucleus, and $\Sigma\chi_c$ is the sum of Pauling electronegativities of the four *cis*-donor atoms. The comparison of the observed and calculated ^{125}Te chemical shifts are shown in Table 4.

This semi-quantitative correlation shows that the shielding of tellurium expectedly decreases with the increasing electronegativity of the donor atoms and can be used to discuss the assignment of the resonance at 294 ppm. The low frequency chemical shift at 294 ppm therefore indicates that both the electronegativity of the donor atom in *trans*-position and that of the four *cis*-donor atoms must be rather low. One possibility for the species giving rise to the observed ^{125}Te chemical shift is *trans*-[$RhCl_2${$Te(CH_2SiMe_3)_2$}$_4$]$^+$ with a Cl^- counter ion (see Table 4). Analogous chalcogenoether complexes are known, as exemplified by [$RhCl_2${o-$C_6H_4(CH_2EMe_2)_2$}$_2$]Y (E = S or Se, Y = PF_6^-; E = Te, Y = Cl^-) [27].

3.4. Formation and isomerism of dinuclear complexes

Whereas there is no report of the crystal structure of $RhCl_3 \cdot 3H_2O$, it can be thought to exist as two isomers: *mer*-[$RhCl_3(OH_2)_3$] and *fac*-[$RhCl_3(OH_2)_3$]. Its reaction with $Te(CH_2SiMe_3)_2$ can be thought to proceed, as follows.

With an excess of $Te(CH_2SiMe_3)_2$ in the reaction (the metal-to-ligand molar ratio of 1:3½), the resonances of *mer*-[$RhCl_3${$Te(CH_2SiMe_3)_2$}$_3$] (**1**) and *fac*-[$RhCl_3${$Te(CH_2SiMe_3)_2$}$_3$] are observed in the ^{125}Te NMR spectrum. This indicates a straight-forward ligand

substitution reaction of three H_2O ligands in *mer*-$[RhCl_3(OH_2)_3]$ or *fac*-$[RhCl_3(OH_2)_3]$ by three $Te(CH_2SiMe_3)_2$ molecules.

The formation of the dinuclear complexes can be thought to proceed in two steps. The first step involves the formal condensation of the mononuclear $[RhCl_3(OH_2)_3]$ complexes into dinuclear chlorido-bridged complexes [28], and the second step involves the ligand substitution of aqua ligands either by tellane or ethanol

$$2[RhCl_3(OH_2)_3] \rightleftharpoons [Rh_2(\mu\text{-}Cl)_2Cl_4(OH_2)_4] + 2H_2O$$
$$[Rh_2(\mu\text{-}Cl)_2Cl_4(OH_2)_4] + 4L \rightleftharpoons [Rh_2(\mu\text{-}Cl)_2Cl_4L_4] + 4H_2O$$

By using the argumentation of Cotton et al. [21], there are nine possible isomers of $[Rh_2(\mu\text{-}Cl)_2Cl_4(OH_2)_4]$ assuming that the oxidation state of both rhodium centers is +III. Their formation from *mer*- and *fac*-isomers of $[RhCl_3(OH_2)_3]$ is shown in Fig. 7. As discussed above, the reaction of $[RhCl_3(OH_2)_3]$ with an excess of $Te(CH_2SiMe_3)_2$ affords mostly *mer*-$[RhCl_3\{Te(CH_2SiMe_3)_2\}_3]$ (**1**) with only some *fac*-isomer. It can therefore be concluded that *mer*-$[RhCl_3(OH_2)_3]$ is likely to be the major reactant in the reaction solution. Thus, only the five condensation reactions involving two *mer*-$[RhCl_3(OH_2)_3]$ complexes are relevant for the production of dinuclear complexes. The observation of only the isomer **A** in both $[Rh_2(\mu\text{-}Cl)_2Cl_4\{Te(CH_2SiMe_3)_2\}_4]$ (**2**) and $[Rh_2(\mu\text{-}Cl)_2Cl_4\ (OHCH_2CH_3)\{Te(CH_2SiMe_3)_2\}_3]$ (**3**) indicates that only the first condensation reaction in Fig. 7 takes place. The formation of isomer **A** is consistent with the reasoning of Cotton et al. [21].

4. Conclusions

$RhCl_3 \cdot 3H_2O$ was treated with $Te(CH_2SiMe_3)_2$ in different molar ratios. By using an excess of the tellane (metal-to-ligand molar ratio of 1:3½), a mononuclear *mer*-$[RhCl_3\{Te(CH_2SiMe_3)_2\}_3]$ (**1**) was observed as the main product. By reducing the metal-to-ligand molar ratio, dinuclear $[Rh_2(\mu\text{-}Cl)_2Cl_4\{Te(CH_2SiMe_3)_2\}_4]$ (**2**) was obtained in addition to **1**. Further reduction of the metal-to-ligand ratio resulted in the formation of $[Rh_2(\mu\text{-}Cl)_2Cl_4(OHCH_2CH_3)\{Te(CH_2SiMe_3)_2\}_3]$ (**3**). The complexes were characterized by X-ray crystallography and ^{125}Te NMR spectroscopy.

The addition of $Te(CH_2SiMe_3)_2$ to the solution of *mer*-$[RhCl_3(SMePh)_3]$ (**4**) yielded a mixture of **4**, *mer*-$[RhCl_3\{Te(CH_2SiMe_3)_2\}_3]$ (**1**), and *mer*-$[RhCl_3(SMePh)\{Te(CH_2SiMe_3)_2\}_2]$ (**5**·). The complexes **4** and **5** · ½EtOH were also characterized by X-ray crystallography and NMR spectroscopy.

The trends in the ^{125}Te chemical shifts and $^1J_{Te\text{-}Rh}$ coupling constants enabled the tentative identification of *fac*-$[RhCl_3\{Te(CH_2SiMe_3)_2\}_3]$ and *trans*-$[RhCl_2\{Te(CH_2SiMe_3)_2\}_4]Cl$ among the reaction products.

Acknowledgment

Financial support from Academy of Finland and the Ministry of Education (L.V.) is gratefully acknowledged.

Appendix A. Supplementary material

CCDC 713502, 713503, 713504, 713505 and 713506 contain the supplementary crystallographic data for this paper. These data can be obtained free of charge from The Cambridge Crystallographic Data Centre via www.ccdc.cam.ac.uk/data_request/cif. Supplementary data associated with this article can be found, in the online version, at doi:10.1016/j.jorganchem.2009.02.001.

References

[1] S.G. Murray, F.R. Hartley, Chem. Rev. 81 (1981) 365.
[2] H.J. Gysling, Coord. Chem. Rev. 42 (1982) 133.
[3] H. Gysling, in: S. Patai, Z. Rappoport (Eds.), The Chemistry of Organic Selenium and Tellurium Compounds, vol. I, Wiley, New York, 1986, pp. 679–855.
[4] E.G. Hope, W. Levason, Coord. Chem. Rev. 122 (1993) 109.
[5] W. Levason, S.D. Orchard, G. Reid, Coord. Chem. Rev. 225 (2002) 159.
[6] S.A. Gardner, J. Organomet. Chem. 190 (1980) 289.
[7] W. Levason, G. Reid, V.A. Tolhurst, J. Chem. Soc., Dalton Trans. (1998) 3411.
[8] T. Kemmitt, W. Levason, R.D. Oldroyd, M. Webster, Polyhedron 11 (1992) 2165.
[9] K. Badyal, W.R. McWhinnie, H.L. Chen, T.A. Hamor, J. Chem. Soc., Dalton Trans. (1997) 1579.
[10] M.P. Devery, R.S. Dickson, B.W. Skelton, A.H. White, Organometallics 18 (1999) 5292.
[11] W. Levason, S.D. Orchard, G. Reid, J.M. Street, J. Chem. Soc., Dalton Trans. (2000) 2537.
[12] A.J. Barton, W. Levason, G. Reid, A.J. Ward, Organometallics 20 (2001) 3644.
[13] M. Hesford, W. Levason, S.D. Orchard, G. Reid, J. Organomet. Chem. 649 (2002) 214.
[14] H.J. Gysling, H.R. Luss, D.L. Smith, Inorg. Chem. 18 (1979) 2696.
[15] L. Vigo, R. Oilunkaniemi, R.S. Laitinen, Eur. J. Inorg. Chem. (2008) 284.
[16] L. Vigo, M.J. Poropudas, R. Oilunkaniemi, R.S. Laitinen, J. Organomet. Chem. 693 (2008) 557.
[17] R. Oilunkaniemi, L. Vigo, M.J. Poropudas, R.S. Laitinen, Phosphorus Sulfur Silicon Relat. Elem. 183 (2008) 1046.
[18] H.C.E. McFarlane, W. McFarlane, J. Chem Soc., Dalton Trans. (1973) 2416.
[19] A. Altomare, G. Cascarano, C. Giacovazzo, A. Gualardi, J. Appl. Crystallogr. 26 (1993) 343.
[20] G.M. Sheldrick, Acta Crystallogr. 64A (2008) 112.
[21] F.A. Cotton, S.-J. Kang, S.K. Mandal, Inorg. Chim. Acta 206 (1993) 29.
[22] J.A. Muir, M.M. Muir, A.J. Rivera, Acta Crystallogr. 30B (1974) 2062.
[23] A. Abbasi, M. Habibian, M. Sandström, Acta Crystallogr. 63E (2007) m1904.
[24] P.D. Clark, J.H. Machin, J.F. Richardson, N.I. Dowling, J.B. Hyne, Inorg. Chem. 27 (1988) 3526.
[25] M. Parvez, J.F. Fait, P.D. Clark, C.G. Jones, Acta Crystallogr. 49C (1993) 383.
[26] J. Emsley, The Elements, 3rd ed., Clarendon Press, Oxford, 1988. p. 292.
[27] W. Levason, M. Nirwan, R. Ratnani, G. Reid, N. Tsoureas, M. Webster, Dalton Trans. (2007) 439.
[28] A.V. Belyaev, M.A. Fedotov, V.I. Korsunskii, A.B. Venediktov, S.P. Khranenko, Koord. Khim. 10 (1984) 911.
[29] S.E. Boyd, L.D. Field, T.W. Hambley, Acta Crystallogr. 50C (1994) 1019.